Two-surface-plasmon-polariton-absorption based lithography using 400 nm femtosecond laser

Yunxiang Li, Fang Liu,[a] Yu Ye, Weisi Meng, Kaiyu Cui, Xue Feng, Wei Zhang, and Yidong Huang[b]
Department of Electronic Engineering, Tsinghua National Laboratory for Information Science and Technology, Tsinghua University, Beijing 100084, China

(Received 3 December 2013; accepted 13 February 2014; published online 26 February 2014)

The two-surface-plasmon-polariton-absorption (TSPPA) at the vacuum wavelength of 400 nm is observed, and the subwavelength lithography, by using this nonlinear phenomenon, is demonstrated. Resist patterns with the period of ~138 nm have been obtained by exciting the SPP at the Al/resist interface with the 400 nm femtosecond laser. By altering the exposure time, the exposure linewidth reduces from ~90 nm to ~55 nm, which explores the ability of the TSPPA based lithography at the short wavelength. The factors limiting the performance of the proposed TSPPA based lithography are discussed in detail. © *2014 AIP Publishing LLC*. [http://dx.doi.org/10.1063/1.4866870]

Surface plasmon polariton (SPP) is a transverse magnetic surface wave oscillating with the collective electrons along a metal-dielectric interface,[1] which has attracted wide interests and intensive studies in recent decades. The wavelength of SPP could be much shorter than that of the lightwave with the same frequency, which makes it possible to carry the subwavelength information. Besides, its field could be highly concentrated near the metal/dielectric interface leading to the extreme field confinement and then the intense interaction with the surrounding media. These unique properties are promising for fighting against the optical diffraction limit, especially in the application of photolithography. For example, SPP generated by high-index prisms,[2,3] period gratings,[4–6] or other nano-structures[7,8] can form interference patterns with the linewidth of SPP-wavelength scale. An extremely tiny light spot realized by the localization/concentration of SPP with the help of nanotips,[9,10] focus lens,[11] or other patterned metal structures[12,13] was also widely applied in nanopatterning. On the other hand, photoresists with special features have been extensively explored aiming to further beat the diffraction limit. Benefiting from the strong field enhancement induced by SPP, nonlinear interactions or thermal effects[11,13–15] could now be possibly useful in lithography applications. It has been reported that resist patterns with 22 nm half-pitch resolution were achieved by combining SPP focusing and the thermal effect in resists, which enabled a high-throughput maskless plasmonic lithography.[11]

Recently, our group has proposed a plasmonic lithography method based on two-SPP-absorption (TSPPA) and demonstrated the TSPPA phenomenon using the 800 nm femtosecond laser.[6] The ability of linewidth control based on the TSPPA threshold was demonstrated by altering the exposure power. However, the absolute linewidth in our previous work was limited by the relatively long exposure wavelength. The absolute linewidth could be further reduced if the TSPPA can be realized with the shorter-wavelength exposure source.

In this work, we demonstrate the TSPPA, as well as, the nanolithography at the wavelength of 400 nm. By illuminating the nano-slit pairs in the Al thin film with the 400 nm femtosecond laser, SPP interference patterns at the Al/resist interface are effectively excited and further result in the TSPPA in the deep-ultraviolet (DUV) resist. The resist patterns with the linewidth varying from ~90 nm to ~55 nm are demonstrated by altering the exposure doses. The factors that limit the performance of the proposed TSPPA lithography are also discussed in detail. The nano-slits with curved ends are proposed to improve the interference pattern.

To realize the TSPPA and the lithography at the short wavelength, i.e., $\lambda_0 = 400$ nm, there are three key factors: (1) The metallic material should be able to support the SPP wave at the operating wavelength. Taking the SPP at the metal/resist interface for example, the dielectric constants of metal and resist should meet the relation: $\mathrm{Re}(\varepsilon_{metal}) + \varepsilon_{resist} < 0$. Here, we choose Aluminum $(\varepsilon_{Al} = -25 + 4.1 \times i)$[16] as the metal material, which could support the SPP wave at $\lambda_0 = 400$ nm with relatively low propagation loss and further give rise to the obvious interference pattern. It is worth noting that, not limited to the specific case in this paper, various plasmonic structures with different metal materials could be possibly applied in the TSPPA based lithography scheme, as long as the issue of the metal loss is effectively addressed; (2) The femtosecond pulse at the short wavelength with enough power is needed for efficiently activating the nonlinear absorption in the resist. Here, the 400 nm femtosecond pulses are effectively generated by the frequency doubling of 800 nm femtosecond pulses via the nonlinear crystal; (3) The photoresist should be suitable for TSPPA at the short wavelength. It means that the photoresist should be transparent to the light at the operating wavelength λ_0 and at the same time be absorptive at $\lambda_0/2$ for the single-photon photochemical process.[6]

The schematic of the lithography method is shown in Fig. 1(a). The Aluminum is chosen as the metal material according to the above analysis. Different from our previous work,[6] here nano-slits instead of nano-gratings are adopted to excite the SPP at the Al/resist interface. The excitation of

a)liu_fang@mail.tsinghua.edu.cn
b)yidonghuang@tsinghua.edu.cn

 © 2014 AIP Publishing LLC

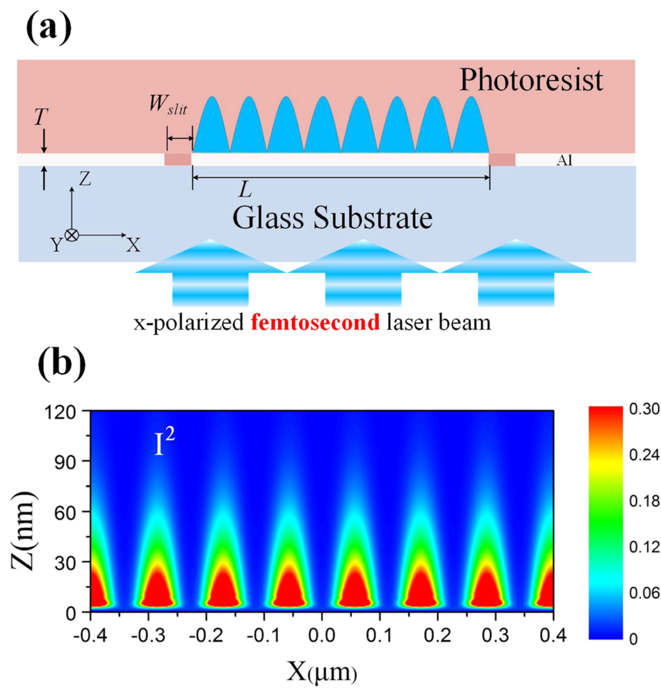

FIG. 1. (a) Schematic of the TSPPA based lithography under the exposure of the femtosecond laser of $\lambda_0 = 400$ nm. (b) The I^2 $(=|E|^4)$ distribution of the SPP interference field induced by nano-slits.

SPP by the nano-slits has been calculated by the Finite-difference time-domain (FDTD) method. Figure 1(b) shows the square intensity distribution ($I^2 = |E|^4$) of the interference pattern generated by the nano-slits. The simulation result indicates that the SPP excitation efficiency with nano-slits is about 40% of that with nano-gratings. Although the excitation efficiency of SPP with nano-gratings is relatively higher than that with nano-slits, the nano-gratings whose period should be approximately equal to the SPP wavelength for effective excitation require more precise fabrication and more fabrication time. Nano-slits could greatly simplify the fabrication process and could possibly excite the SPP at different wavelength. The decrease of SPP intensity due to the low excitation efficiency could be simply compensated by increasing the power of input light. And the quality of the lithography pattern would not suffer from this efficiency issue. Besides, the SPP excitation efficiency using nano-slits could be further optimized by adjusting the slit width and depth.[17] It is worth noting that any SPP modes excited by various structure could be applied in the TSPPA bases lithography, and the SPP excitation efficiency should be taken into account in the practical application.

To realize the SPP mask shown in Fig. 1(a), a 100 nm-thick Al film with average roughness of ~3 nm is deposited on the flat quartz substrate by electron beam evaporation. Nano-slits with the width of $w_{width} = \sim 80$ nm and the interval of $L = \sim 2.3\ \mu$m are patterned into the Al film by a focused-ion-beam system (FIB, Tescan Lyra), as shown in Fig. 2. Then, a thin resist layer is spin-coated on the Al film. The 400 nm femtosecond laser is focused on the sample with its polarization perpendicular to the length direction of nano-slits.

As shown in the experiment setup in Fig. 3(a), a nonlinear crystal (β-BaB_2O_4, BBO) is used to convert input 800 nm

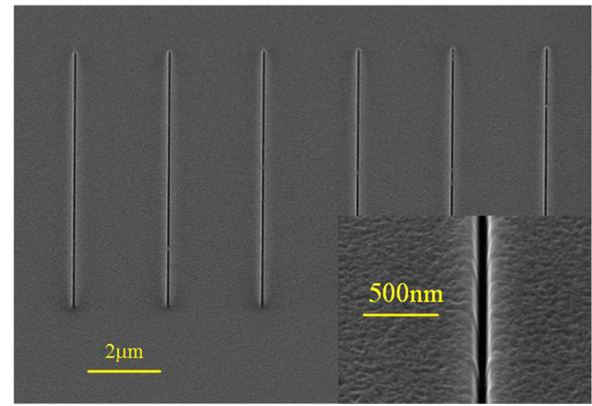

FIG. 2. The SEM pictures of nano-slits by FIB milling.

pulses into 400 nm femtosecond pulses. The angle between the incident light and the BBO crystal is carefully adjusted to achieve the maximum conversion efficiency. The remaining 800 nm light is filtered out, and the measured spectrum of the light coming out from the filter is shown as the red line in Fig. 3(b). In order to realize effective TSPPA at 400 nm wavelength, here, we choose a DUV resist (ma-N2400, Micro resist) whose absorption spectrum is below 330 nm, as shown by the blue dashed line in Fig. 3(b),[18] which meets the requirement of the TSPPA as mentioned above.

At first, the sample is exposed for 8 s at the average power of 50 mW and then is developed with ma-D 525 for 8 s. The atomic force microscope (AFM) and the scanning electron microscope (SEM) results of the resist strips are presented in Figs. 4(a) and 4(b), respectively. The resist strips indicated by green dashed lines in Figs. 4(a) and 4(b) are caused by the electromagnetic energy straightly coming out of nano-slits. The periodic resist strips induced by the TSPPA could be clearly seen between the green dashed lines. In order to precisely estimate the period of the obtained resist strips, we perform 1D Fourier transform to the measured AFM result along the x axis. The result reveals that the average period of resist strips is about 138 nm. Figure 4(c) shows

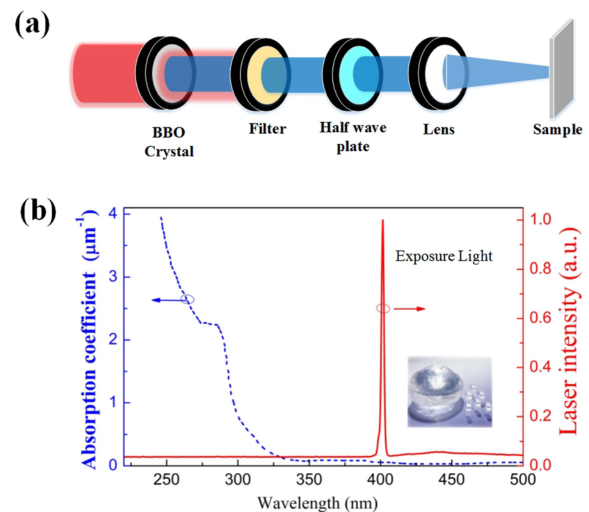

FIG. 3. (a) The experiment setup for the TSPPA based lithography with the femtosecond laser of $\lambda_0 = 400$ nm. (b) The measured spectrum of the 400 nm femtosecond laser coming out from the filter (red solid line) and the UV/vis absorption of the unexposed DUV resist (ma-N2400) (blue dashed line).

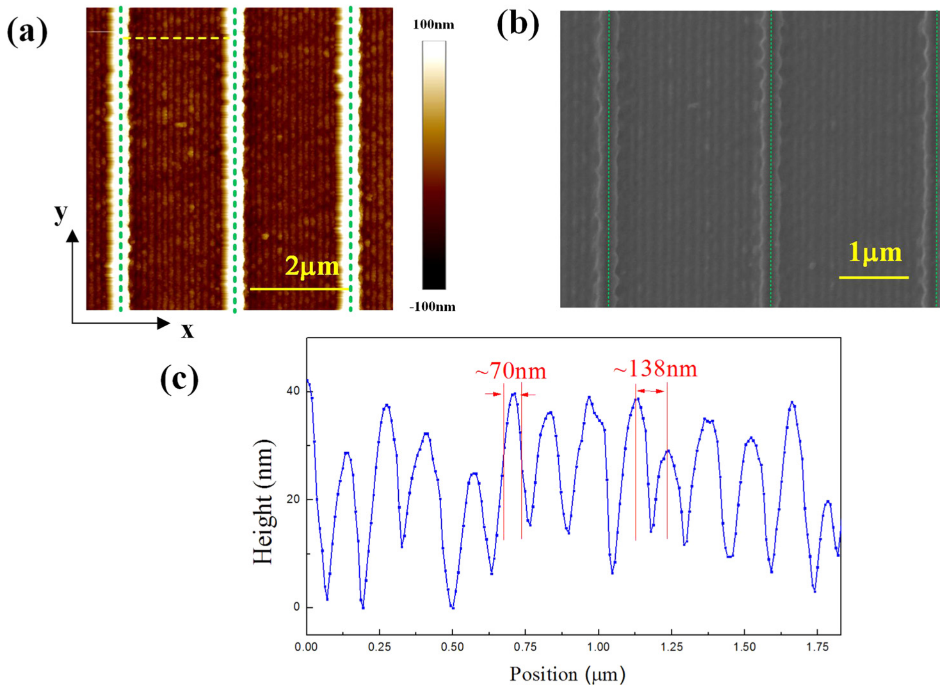

FIG. 4. (a) The AFM result and (b) the SEM picture of the resist pattern for the exposure time of 8 s. (c) The surface profile of the resist pattern along the yellow dashed line in Fig. 4(a). The dashed green lines in Figs. 4(a) and 4(b) indicate the resist strips resulting from the electromagnetic energy straightly coming out of nano-slits.

the pattern profile along the yellow dashed line in Fig. 4(a). The linewidth of the resist strips is not quite uniform due to the reasons of both the imperfect fabrication process and the scattering and interference of other SPP modes, which will be discussed in detail later. Hence, in order to objectively evaluate the exposure linewidth, strips profiles at different locations in Fig. 4(a) have been sampled, and the full width at half maximum of those strips have been calculated to obtain the average linewidth.

By applying the above criterion, the average exposure linewidth of ~70 nm is obtained. In the previous paper, it was proposed that the exposure linewidth can be controlled by manipulating the exposure dose. Here, Fig. 5 shows the linewidth of the resist patterns for the exposure time of 20 s, 15 s, 8 s, 5 s, and 3 s. It is indicated that the periods of the resist strips remain the same for different exposure time. However, the average exposure linewidth reduces from ~90 nm to ~55 nm as the exposure time decreases, which shows that the TSPPA based lithography has the ability of the linewidth control by altering the exposure dose. It is worth noting that,

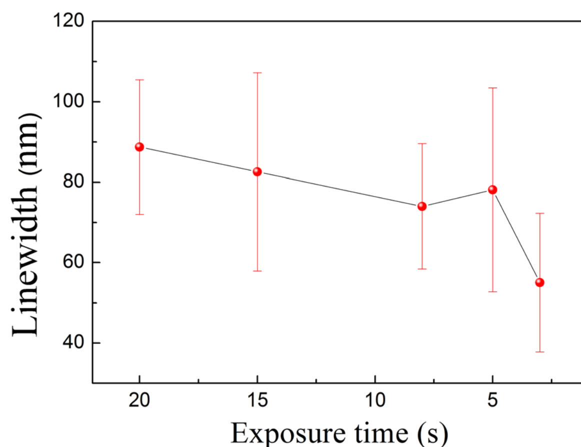

FIG. 5. The average exposure linewidth for different exposure time.

although the linewidth reduction could also be achieved by controlling the exposure dose and the development condition in the traditional lithography, the photochemical reaction here induced by a nonlinear absorption of two SPP could provide a more flexible and powerful way for controlling the exposure linewidth due to its pronounced power threshold effect.[6]

The above results demonstrate the TSPPA based lithography using 400 nm exposure light, in which the linewidth obviously decreases by reducing the exposure dose. However, the resist strips suffer from the rough line edge and the low uniformity of the strips, which results in the difficulty for precise evaluation of the exposure linewidth and prevents the TSPPA based lithography from the better performance. The unwanted scattering and interference of other SPP modes induced by the excitation structures and the imperfect fabrication process are the main factors that deteriorate the interference pattern.

First, the slit in our excitation structure, especially the end of the nano-slit, could diffract the incident light into various wave-vector components with different magnitudes and directions. Some of these components would couple into several SPP modes supported in the structure by compensating the wave-vector differences.[19] Besides the SPP mode along x-axis (indicated by red arrows in Fig. 6(a)) which results in the interference pattern in our experiment, the SPP modes along other directions have also been excited near the end of the nano-slit (indicated by black arrows in Fig. 6(a)). And these SPP modes would overlap with the interference patterns generated by the counter-propagating SPP perpendicular to the nano-slits and lead to the nonuniform strips. To minimize this non-uniformity of the periodic strips, here we introduce a curved nano-slit at the end of the straight nano-slit as shown in the inset of Fig. 6(b), to suppress the excitation of SPP modes indicated by the black arrows in Fig. 6(a). Figure 6(b) shows the simulated interference patterns excited by nano-slits with curved ends of 5 μm-radius, which indicates that the excitation of SPP modes along other directions at the

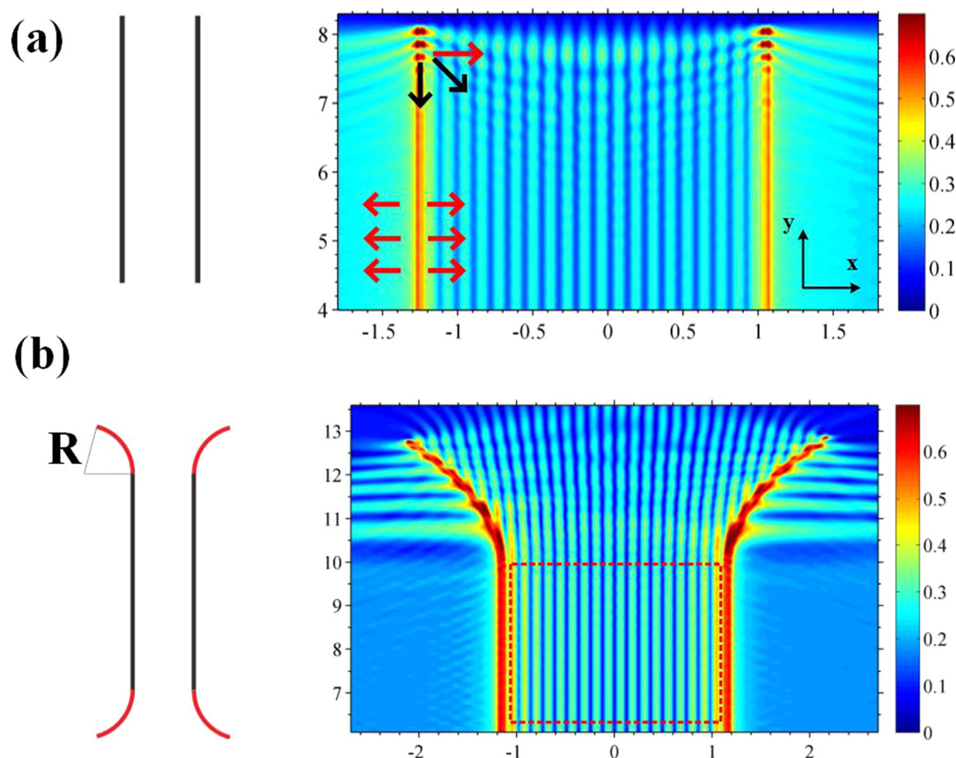

FIG. 6. (a) The interference pattern generated by the straight nano-slits. (b) The simulated interference patterns by the nano-slits with curved ends of 5 μm-radius.

straight-slits region (dashed rectangle in Fig. 6(b)) has been suppressed and the uniformity of the patterns are improved. Second, the imperfect fabrication process also deteriorates the interference pattern. As shown in the inset of Fig. 2, the rough edges of nano-slits are introduced by the FIB process, which would cause the scattering of excited SPP and disturb the final interference pattern. The resist strips indicated by the green dashed lines in Figs. 4(a) and 4(b) show the rough edges, which directly reveals the rough-edge nano-slits beneath them. Besides, the roughness of the Al thin film is vital to our lithography result. The rough Al surface might also scatter the propagating SPP and deteriorate the field distribution. Thus, to get high-quality resist strips, the fabrication technique of metal mask should be improved.

Moreover, in order to further decrease the lithography linewidth, the TSPPA based lithography could be applied at even shorter wavelength, for example, 193 nm or EUV, as long as the material issue (such as metal supporting the SPP, suitable photoresist) could be addressed. Besides, other SPP modes with smaller wavelength could also be used to reduce the lithography linewidth. For instance, the slot SPP mode, which exists in the metal-dielectric-metal structure and has smaller effective wavelength, could also be useful in the lithography application.[20]

In summary, the key factors for realizing TSPPA at the short wavelength are discussed, and the ability of TSPPA based nanolithography is further explored by using the 400 nm femtosecond laser pulse. The resist patterns with the period of ~138 nm are demonstrated, and the exposure linewidth reduces from ~90 nm to ~55 nm by altering the exposure time when the strips period remains the same. The limitations for better performance of the proposed lithography, namely, the unwanted SPP modes induced by the excitation structures or the imperfect fabrication process, are also discussed. It is expected that the further development of the proposed TSPPA based lithography at shorter wavelength would provide a promising way for subwavelength patterning.

This work was supported by the National Basic Research Programs of China (973 Program) under Contract Nos. 2013CBA01704, 2010CB327405, and 2011CBA00608, and the National Natural Science Foundation of China (NSFC-61036011, 61107050, 61036010, and 61321004).

[1]S. A. Maier, *Plasmonics: Fundamentals and Applications* (Springer, 2007).
[2]K. V. Sreekanth and V. M. Murukeshan, Appl. Phys. A: Mater. Sci. Process. **101**, 117 (2010).
[3]X. Guo, J. Du, Y. Guo, and J. Yao, Opt. Lett. **31**, 2613 (2006).
[4]Z. W. Liu, Q. H. Wei, and X. Zhang, Nano Lett. **5**, 957 (2005).
[5]X. Luo and T. Ishihara, Appl. Phys. Lett. **84**, 4780 (2004).
[6]Y. Li, F. Liu, L. Xiao, K. Cui, X. Feng, W. Zhang, and Y. Huang, Appl. Phys. Lett. **102**, 063113 (2013).
[7]N. Fang, H. Lee, C. Sun, and X. Zhang, Science **308**, 534 (2005).
[8]H. Liu, B. Wang, L. Ke, J. Deng, C. C. Choy, M. S. Zhang, L. Shen, S. A. Maier, and J. H. Teng, Adv. Funct. Mater. **22**, 3777 (2012).
[9]Y. Wang, W. Srituravanich, C. Sun, and X. Zhang, Nano Lett. **8**, 3041 (2008).
[10]X. Wei, C. Du, X. Dong, X. Luo, Q. Deng, and Y. Zhang, Opt. Express **16**, 14404 (2008).
[11]L. Pan, Y. Park, Y. Xiong, E. Ulin-Avila, Y. Wang, L. Zeng, S. Xiong, J. Rho, C. Sun, D. B. Bogy, and X. Zhang, Sci. Rep. **1**, 175 (2011).
[12]W. Srituravanich, N. Fang, C. Sun, Q. Luo, and X. Zhang, Nano Lett. **4**, 1085 (2004).
[13]K. Ueno, S. Takabatake, K. Onishi, H. Itoh, Y. Nishijima, and H. Misawa, Appl. Phys. Lett. **99**, 011107 (2011).
[14]A. Sundaramurthy, P. J. Schuck, N. R. Conley, D. P. Fromm, G. S. Kino, and W. E. Moerner, Nano Lett. **6**, 355 (2006).
[15]Z. Gan, Y. Cao, R. A. Evans, and M. Gu, Nat. Commun. **4**, 2061 (2013).
[16]A. D. Raki, Appl. Opt. **34**, 4755 (1995).
[17]P. Lalanne, J. Hugonin, and J. Rodier, J. Opt. Soc. Am. A **23**, 1608 (2006).
[18]Negative Tone Photoresist Series ma-N 2400 Datasheet, Micro Resist.
[19]Z. Liu, Y. Wang, J. Yao, H. Lee, W. Srituravanich, and X. Zhang, Nano Lett. **9**, 462 (2009).
[20]W. Ge, C. Wang, Y. Xue, B. Cao, B. Zhang, and K. Xu, Opt. Express **19**, 6714 (2011).